TITLE

Multimodel Analysis of the Atmospheric Response to Antarctic Sea Ice Loss at Quadrupled CO2

AUTHORS

Ayres, HC; Screen, JA

JOURNAL

Geophysical Research Letters

DEPOSITED IN ORE

04 September 2019

Multi-Model Analysis of the Atmospheric Response to Antarctic Sea Ice Loss at Quadrupled CO_2

H. C. Ayres[1], J. A. Screen[1]

[1] College of Engineering, Mathematics and Physical Sciences, University of Exeter, Exeter EX4 4QE, UK.

Corresponding author: Holly Ayres (ha392@exeter.ac.uk)

Key Points:

- Projected Antarctic sea-ice loss weakens the tropospheric westerly jet and favors the negative phase of the Southern Annular Mode (SAM).
- Negative SAM response to sea-ice loss damps but does not fully offset the positive SAM response to increased CO_2.
- Sea-ice loss causes near-surface warming over the high-latitude Southern Ocean, but warming does not penetrate the Antarctic continent.

Abstract

Antarctic sea-ice cover is projected to significantly decrease by the end of the 21st century if greenhouse gas concentrations continue to rise, with potential consequences for Southern Hemisphere weather and climate. Here, we examine the atmospheric response to projected Antarctic sea-ice loss at quadrupled CO_2, inferred from eleven CMIP5 models. Our study is the first multi-model analysis of the atmospheric response to Antarctic sea-ice loss. Projected sea-ice loss enhances the negative phase of the Southern Annular Mode (SAM), which slightly damps the positive SAM response to increased CO_2, particularly in spring. The negative SAM response largely reflects a weakening of the eddy-driven jet, and to a lesser extent, an equatorward shift of the jet. Sea-ice loss induces near-surface warming over the high-latitude Southern Ocean, but warming does not penetrate over the Antarctic continent. In spring, we find multi-model evidence for a weakened polar stratospheric vortex in response to sea-ice loss.

Plain Language Summary

Increasing greenhouse gases through human activities are predicted to cause a decrease in Antarctic sea-ice cover by the end of the century. If this happens, it is unknown what the impacts on Southern Hemisphere weather and climate could be. The aim of this study was to use simulations from eleven climate models to explore the potential consequences of future Antarctic sea-ice loss. We analyzed model simulations with CO_2 quadrupled from pre-industrial levels, which led to large reductions in Antarctic sea-ice. We found that sea-ice loss led to warmer temperatures in the lowermost atmosphere over the Southern Ocean, but that this warming did not penetrate the Antarctic continent. Sea-ice loss also had an impact on the predominantly westerly winds that encircle Antarctica, causing them to weaken. Climate models have some

difficulties in representing Antarctic sea ice, and as a result, projections of Antarctic sea ice are highly uncertain. Our results imply that reducing uncertainties in projections of Antarctic sea ice may lead to better forecasts of future changes in Southern Hemisphere weather and climate.

1. Introduction

Accurate satellite records of polar sea ice began in 1979. Since this time, annual-mean Arctic sea ice extent (SIE) has decreased significantly by ~960 thousand square kilometers per decade (Fetterer et al., 2017), whereas annual-mean Antarctic SIE has increased by a lower, but still significant, ~54 thousand square kilometers per decade (Fetterer et al., 2017). In austral spring 2016, Antarctic SIE decreased at an abnormal rate, 18% quicker than in any previous melting season in the satellite record and 46% quicker than the average melt rate (Turner et al., 2017). Possible explanations for the sudden 2016 decline include influences from the El Niño Southern Oscillation (ENSO) and an enhanced zonal wavenumber-3 pattern of the westerly jet (Schlosser et al., 2017; Stuecker et al., 2017). In addition, new research has shown that the rapid sea-ice loss led to ocean warming and enhanced upward propagation of planetary scale waves, triggering a stratospheric warming event, subsequently influencing the westerly jet and further enhancing ice melt (Meehl et al., 2019; Wang et al., 2019). Since 2016, Antarctic SIE has tracked well below it's long-term average. It is unclear if this dramatic reduction is temporary or if the Southern Hemisphere sea ice is entering a new era of decline (Ludescher et al., 2018).

The Coupled Model Intercomparison Project Phase 5 (CMIP5) climate models simulate, on average, a loss of sea ice over the historical period and not an increase as has been observed. This disagreement between observations and models remain poorly understood (Turner et al., 2013), but possible explanations include internal climate variability (Polvani & Smith, 2013), model biases (e.g Bracegirdle et al., 2013; Bracegirdle et al., 2018; Holland et al., 2017; Lecomte et al., 2016; Purich et al., 2016; Roach et al., 2018; Schroeter et al., 2017; Turner et al., 2013) or unresolved processes in models such as ice-sheet-ocean interactions. The same models project that Antarctic sea ice will continue to decline significantly by 2100 (e.g. Collins et al., 2013; Vaughan, 2013) if greenhouse gas concentrations continue to rise, although there is significant divergence between models in the magnitude of the projected decline. Nevertheless, future trends in Antarctic sea ice may have numerous impacts on the surrounding atmosphere.

It is well understood that Arctic sea-ice loss is influencing high latitude weather and climate in the Northern Hemisphere, with thermodynamically induced warming and moistening of the atmosphere, amongst other changes. There is also emerging evidence that reduced Arctic sea ice may influence the large-scale atmospheric circulation, for example, through weakening of the mid-latitude westerly winds (e.g., Peings & Magnusdottir, 2014) and a negative shift in the North Atlantic Oscillation index (Blackport & Kushner, 2016; Deser et al., 2015; Kim et al., 2014; Peings & Magnusdottir, 2014; Screen & Simmonds, 2013; Screen et al., 2013). Several review papers have been published on the atmospheric response to Arctic sea-ice loss, including Cohen et al. (2014), Vavrus (2018) and Screen et al. (2018). The potential for such atmospheric responses to Antarctic sea-ice loss has been less well studied.

The observed gradual growth of Antarctic sea ice has been suggested to result in a slight poleward shift of the tropospheric jet in the austral winter months (Smith et al., 2017). Raphael et al. (2011) suggested that negative summer sea ice anomalies were linked to a more negative Southern Annular Mode (SAM) index and vice versa. Studies examining the atmospheric response to projected Antarctic sea-ice loss have revealed contrasting results, with Kidston et al. (2011) finding no significant impacts whereas Bader et al. (2013) and Menéndez et al. (1999) both found an equatorward shift of the tropospheric jet. More recently, England et al. (2018)

used the WACCM4 model to compare impacts of Arctic and Antarctic sea-ice loss. These authors found a significant equatorward shift of the eddy-driven jet in response to sea-ice loss in either hemisphere. They also found that the tropospheric and stratospheric responses to Antarctic sea-ice loss were of smaller amplitude, more vertically confined and with less seasonal variation than in response to Arctic sea-ice loss.

In this paper, we use the CMIP5 multi-model ensemble to assess the atmospheric response to projected Antarctic sea-ice loss across the Southern Hemisphere. Our study is the first to look at the impacts of projected Antarctic sea-ice loss using a multi-model ensemble.

2. Data and Methods

Zappa et al. (2018) introduced a novel method of estimating the response to projected sea-ice loss using existing CMIP5 simulations. Their study applied this method to analyze the wintertime atmospheric response to projected Arctic sea-ice loss and in particular, that of the North Atlantic jet. Here, we apply a very similar methodology to examine the seasonal atmospheric response to Antarctic sea-ice loss when the CO_2 concentration is quadrupled. We use output from 11 climate models (Table S4), which had all the required experiments. Prior to analysis and to facilitate averaging across models, data were interpolated onto a T42 grid.

To estimate the coupled climate response to quadrupled CO_2, we compare 100-year means (years 50-150) from the CMIP5 ‘abrupt4xCO2’ simulations to 100-year climatologies from the preindustrial control simulations (‘piControl’). We chose to use ‘abrupt4xCO2’ rather than any of the Representative Concentration Pathway (RCP) experiments (Zappa et al. (2018) used

RCP8.5), to avoid the complicating influences of non-CO_2 climate drivers, such as ozone and aerosols, which are included in the RCPs but not in ‘abrupt4xCO2’. Furthermore, the use of ‘abrupt4xCO2’ results in scaling factors (described below) closer to unity, which reduces our reliance on the assumption of linear scalability of the atmospheric response to SST warming and CO_2 increase. The atmospheric response to quadrupled CO_2 was estimated by comparing 30-year means (years 1979-2008) from the ‘amip4xCO2’ simulations to those in the ‘amip’ simulations. Likewise, the atmospheric response to SST warming was estimated by comparing 30-year means from the ‘amipFuture’ and ‘amip’ simulations. The ‘amip’ simulations were prescribed with observed variability in sea ice concentrations, sea surface temperatures (SST) and atmospheric composition for the period 1979-2008. The ‘amipFuture’ simulations are identical to ‘amip’, except that they have added SST perturbations derived from the CMIP3 ‘abrupt4xCO2’ multi-model response, scaled to have a global average warming of 4 K. The ‘amip4xCO2’ simulations are identical to ‘amip’ except that the CO_2 concentration was quadrupled. Sea ice is kept unchanged at present day values in both ‘amip4xCO2’ and ‘amipFuture’, so is identical to that in ‘amip’. The fact that sea ice is unchanged, but that either SST or CO_2 is changed, allows for the response to sea-ice loss to be estimated as the residual between the coupled climate response (‘abrupt4xCO2’ minus ‘piControl’) and the combined and scaled atmospheric responses to SST warming and quadrupled CO_2, termed $AMIP_{sst+co2}$, where:

$$AMIP_{sst+co2} - AMIP = k_{sst}.(AMIP_{Future} - AMIP) + k_{co2}.(AMIP_{4xCO2} - AMIP) \qquad (1)$$

Here, k_{sst} is the temperature scaling factor derived as the ratio of tropical 30°S-30°N zonal-mean warming at 100-300 hPa in ‘amipFuture’ (relative to ‘amip’) to that in ‘abrupt4xCO2’ (relative to ‘piControl’). This scaling was chosen to capture the tropical upper tropospheric warming, which is a dominant feature (or ‘fingerprint’) of global warming. k_{sst} was calculated for each of the eleven models, with an average of $k_{sst} = 0.8047$. k_{co2} is the scaling of CO_2 radiative forcing, which, for our purposes is unity. Hereafter we refer to the multi-model-mean difference between the coupled climate response and $AMIP_{sst+co2}$, as the inferred response to sea-ice loss. Our estimate of the inferred response to sea-ice loss is derived as a residual from coupled model experiments and so, it includes any effects of ocean coupling on the response to sea-ice loss (see, e.g., Deser et al., 2015). However due to the scaling (k_{sst}), we expect that any tropical response to sea-ice loss, and any feedback of sea-ice-induced tropical changes on the extratropics, would be missed by our method and instead apportioned to SST change.

The tropospheric eddy-driven jet shift was calculated using a monthly-mean jet latitude index (Ceppi et al., 2018; Zappa et al., 2018). The zonal average of the monthly-mean climatological zonal wind ($\bar{u}$) at 850hPa was first taken for the Southern Ocean. The jet latitude (ϕ_{jet}) was then defined as the mean latitude (ϕ) of westerlies weighted by the square of the westerly wind speed:

$$\phi_{jet} = \int_{-30^\circ}^{-65^\circ} \phi \bar{u}_0^2 \, d\phi \; / \int_{-30^\circ}^{-65^\circ} \bar{u}_0^2 \, d\phi \qquad (2)$$

$$\overline{u_0}(\phi) = \max(0, \bar{u}(\phi)) \qquad (3)$$

Unless otherwise stated, we use the shorthand ‘jet’ to refer to the tropospheric eddy-driven jet. We define a robust response to be when nine or more of the eleven models have the same signed response as the multimodel mean.

3. Results

In response to quadrupled CO2, Antarctic sea ice concentrations are reduced in all seasons and in all sectors of the Southern Ocean (Figure 1a-d). During the warmer months, sea-ice loss is mostly limited to high southern latitudes, particularly the Weddell and Ross Seas. In the colder months, sea ice reductions are simulated all around Antarctica and extend further to the north, reaching 55 °S in the Atlantic sector. The loss of sea ice is of greatest magnitude in the late austral autumn through to summer (May-December) and of weaker magnitude in the late austral summer and early autumn (January-April). The loss of sea-ice area (Figure 1e) is greatest in September (7.7 × 106 km^2) and least in February (1.6 × 106 km^2).

As would be expected, the loss of sea-ice leads to an increase in the ocean-to-atmosphere heat flux at the ocean surface. Figure 1f shows the area-weighted surface turbulent (sensible plus latent) heat flux response, summed over Southern Hemisphere grid points where the sea-ice concentration differs between the preindustrial and quadrupled CO_2 states. The inferred heat flux response to the sea-ice loss (Figure 1f) is largest in the austral winter (July-September), reaching a maximum of 300 TW in August, and smallest in spring to summer, with a minimum of 50 TW in January. The annual cycle of the surface heat flux response closely follows the annual cycle of sea-ice area loss; although the monthly maximum and minimum heat flux responses occur one month prior to the maximum and minimum sea-ice area loss. The heat flux response peaks in August, despite sea-ice loss being largest in August-September, because the climatological heat flux is at a maximum in July-August (not shown).

Near-surface air temperatures are significantly increased in regions of sea ice loss (Figure 2a-d), consistent with an enhanced ocean-to-atmosphere heat flux. The seasons and geographical regions of greatest warming are consistent with both the magnitude of sea-ice loss and of the surface heat flux response. Warming reaches a maximum of 7.2 K in the Amundsen Sea in austral winter. The near-surface warming does not extent far inland, probably due to the high elevation of the Antarctic continent and predominantly down-slope winds, in agreement with England et al. (2018).

The inferred mean surface level pressure (MSLP) response to sea-ice loss (Figure 2e-h) resembles the spatial pattern of the negative phase of the SAM, with increased MSLP at high latitudes and reduced MSLP in mid-latitudes, particularly in the austral spring and summer. An increase in MSLP is simulated over the Antarctic continent in all seasons. The MSLP response is highly zonally symmetric in spring and summer. In winter, and to a lesser extent in autumn, the ring of reduced MSLP in midlatitudes is punctuated by increased MSLP in the East Pacific sector (i.e., south of Australia and New Zealand). Also, in winter, MSLP is increased in the Amundsen-Bellingshausen Sea, which implies a reduction in the intensity of the Amundsen Sea Low. The inferred response of the westerly wind in the mid-troposphere (500 hPa; Figure 2i-l) is best described as decrease in westerly wind velocity around Antarctica centered at 65 °S and an increase in mid-latitudes centered at 45 °S. This general pattern is simulated in all seasons but is of greatest magnitude in austral spring and summer, consistent with the MSLP response.

Figure 3a-d shows the vertical profile of the inferred zonal-mean air temperature response to sea-ice loss. The near-surface warming previously discussed is confined to the lower troposphere, below 500 hPa. The most notable features of the temperature response aloft are general cooling of the stratosphere across a range of latitudes and seasons, and polar stratospheric warming in austral spring. We suspect the former may be an artifact of method as both SST warming and quadrupled CO2 favor a cooler stratosphere (not shown). The polar stratospheric warming in spring, however, is not seen in the response to either SST warming or quadrupled CO2 and may indicate a weakened stratospheric polar vortex in response to sea-ice loss.

The inferred zonal-mean westerly wind response to sea-ice loss (Figure 3e-h) shows a weakening of the westerly wind at 60 °S, on the poleward flank of the eddy-driven jet, from the surface to the mid-stratosphere in all seasons, but of largest magnitude in austral winter and spring. The weakening of the stratospheric westerly wind at 60 °S is largest in spring and again, suggests a weakened stratospheric polar vortex. In October, the models depict a robust slowdown of stratospheric polar vortex by 4.5 ms^{-1} (~10% of the climatological SPV strength in this month; Figure S3). Throughout the year, but to a lesser degree in autumn, there is strengthened westerly wind at 40 °S, predominantly in the core of the subtropical jet. The tropospheric response is largest when there is a coincident and same-signed stratosphere response, suggesting troposphere-stratosphere coupling. This result is in accordance with previous studies that have suggested increased stratosphere-troposphere coupling in the austral spring when the stratospheric polar vortex breaks down (e.g., Kidston et al., 2015).

Figures 2 and 3 suggest changes in the westerly eddy-driven jet in response to sea-ice loss, which can be better quantified using the jet latitude and jet strength metrics. The inferred eddy-driven jet latitude response (Figure 4a) shows an equatorward shift in August to February, of 1.5 °

latitude at its maximum in December. December and April are the only months when eight models agree on the sign of the jet latitude response, with approximately seven or fewer models agreeing on the sign of the response in other calendar months. The eddy-driven jet strength is decreased from August to December, with the biggest reduction in jet strength of 0.75 ms^{-1} found in November and corroborated by 9 models (Figure 4b). Changes in the SAM index mimic those of jet strength (Figure S3). The simplest dynamical explanation for the eddy-driven jet weakening is the reduction in the near-surface temperature gradient and resultant decreased baroclinicity (Kidston et al., 2011). We note that the jet responses to sea-ice loss are small and, in most months, of opposite sign, compared to those simulated in response to SST and CO_2. The jet strength and in particular, jet latitude responses are less robust than the 500 hPa westerly wind and zonal-mean zonal wind responses described earlier. We posit that more varied jet responses reflect differences in the average latitude of the jet across the models. Models with a more southerly located jet tend to simulate a poleward-shifted jet in response to sea-ice loss, whereas those with a more northerly located jet tend to simulate an equatorward-shifted jet in response to sea-ice loss (Figure 4c). The models that depict a strengthening jet in response to sea-ice loss have their jets too far north, at around 40 °S, at latitudes where the westerly wind increases (Figure 3). The zonal-mean westerly wind decrease is largest at 60 °S (Figure 3), poleward of the mean jet, and thus, the models with more poleward-located jets are also those that simulate the largest reductions in jet strength in response to sea-ice loss (Figure 4d). These relationships are strongest in winter and spring (not shown for other seasons) and are reminiscent of similar dependencies seen for the projected jet response to increased greenhouse gas concentrations (e.g., Kidston and Gerber, 2010; Bracegirdle et al., 2018).

4. Discussion

Our results suggest an overall weakening of the eddy-driven jet and negative shift in the SAM index in response to projected Antarctic sea-ice loss, particularly in austral spring. This result is in broad agreement with past studies using individual models (Bader et al., 2013; England et al., 2018; Menéndez et al., 1999; Raphael et al., 2011; Smith et al., 2017), but we are the first to provide evidence from a multi-model ensemble. The weakening of the eddy-driven jet and negative SAM in response to sea-ice loss counteract, but only partially offset, the projected jet strengthening and positive SAM in response to increased CO_2 (Figure S1, S2). Thus, projected sea-ice loss acts to slightly weaken the jet and SAM response to increased CO_2. We have shown that the SAM response to projected sea-ice loss primarily reflects changes in eddy-driven jet strength and to a lesser extent, changes in jet latitude, consistent with England et al. (2018).

Our results suggest that in many respects, the multi-model-mean response to projected Antarctic sea-ice loss is analogous to that in response to projected Arctic sea-ice loss. Consistent features of the multi-model responses to Arctic and Antarctic include the weakening of the eddy-driven jet, shift towards the negative phase of the annular mode, and weakening of the stratospheric polar vortex, albeit with some differences in seasonality as also noted by England et al. (2018) for one model. One difference between our results and that for the multi-model-mean response to projected Arctic sea-ice loss is that near-surface temperature response to Antarctic sea-ice loss does not extend over the Antarctic continent (Fig. 2), whereas the surface temperature response to Arctic sea-ice loss does spread to the northern high-latitude continents (e.g., Zappa et al., 2018). We speculate the high elevation of Antarctica isolates the continent from the low-level sea-ice-induced warming. In contrast, Krinner et al. (2014) found a large temperature response over the continent in atmosphere-only simulations with prescribed changes in sea ice and SST. This implies that broader SST warming is key to warming over the Antarctic plateau.

Our results suggest a different seasonality to the stratospheric response to projected Antarctic sea-ice loss to that in England et al. (2018). We found a robust multi-model-mean weakening of the stratospheric zonal wind only in spring, whereas in the single model experiments of England et al. (2018), the stratospheric zonal wind was weakened in autumn and winter, but not in spring. The seasonal timing of maximum stratospheric response shown here is more in line with that in response to projected Arctic sea-ice loss. In the Northern Hemisphere, sea-ice loss appears to enhance the upward propagation of planetary scales waves causing a weakening of the polar vortex in late winter or spring (e.g., Kim et al., 2014). However, it is unclear whether this mechanism operates in the Southern Hemisphere and the zonal symmetry of multi-model-mean tropospheric circulation response implies only small changes in upward wave propagation. Further work with dedicated sea-ice perturbation experiments is required to understand the origins of the stratospheric response to Antarctic sea-ice loss.

5. Conclusions

We have undertaken the first multi-model analysis of the atmospheric response to projected Antarctic sea-ice loss. We find some robust aspects of the atmospheric circulation response to sea-ice loss across eleven models, despite large differences between the models in many aspects. Our results suggest that projected sea-ice loss causes a robust weakening of the tropospheric westerly jet and favors the negative phase of the SAM, of greatest magnitude and robustness in austral spring and summer. In these regards, the response to sea-ice loss acts to weakly damp the strengthening westerly jet and positive SAM responses to increased CO_2. We have shown that the SAM response to sea-ice loss primarily reflects a reduction in jet strength and to a lesser extent, an equatorward shift in the jet. In austral spring, we find multi-model evidence for a weakening polar stratospheric vortex and coupling between the stratospheric and tropospheric zonal wind responses. Sea-ice loss induces warming in the lowermost atmosphere over the high-latitude Southern Ocean, but this warming does not penetrate over the Antarctic continent.

Acknowledgments, Samples, and Data

We thank Thomas Bracegirdle for useful discussions and for commenting on an earlier draft of the paper. We acknowledge the World Climate Research Programme Working Group on Coupled Modelling, which is responsible for CMIP, and the modeling groups listed in Table S1 for producing the simulations and making available their output. CMIP data were obtained from the British Atmospheric Data Centre. This study is supported by the "Robust Spatial Projections of Real-World Climate Change" (NERC, Research grant NE/N018486/1) and the University of Exeter.

Figure captions

Multi-model-mean sea ice concentration response to quadrupled CO_2 in austral (a) summer (January-March; JFM), (b) autumn (April-June; AMJ), (c) winter (July-September; JAS) and (d) spring (October-December). The black and grey contours show the sea-ice edge (15% concentration) in the quadrupled and control simulations, respectively. (e) Multi-model-mean sea-ice area (SIA) response to quadrupled CO_2 as a function of calendar month. The right-hand vertical axis (in blue) shows the number of models that have the same signed response as the multimodel mean, with filled dots indicating nine or more models have the same signed response as the multimodel mean and stars indicating fewer than nine models have the same signed response as the multimodel mean. (f) As (e), but for the inferred surface turbulent heat flux response, calculated as the area-weighted surface turbulent (sensible plus latent) heat flux response, summed over Southern Hemisphere grid points where the sea-ice concentration differs between the preindustrial and quadrupled CO_2 states. The heat flux is defined as positive in the upward direction.

Figure 2: Multi-model-mean inferred surface air temperature (TAS) response to Antarctic sea-ice loss in austral (a) summer (January-March; JFM), (b) autumn (April-June; AMJ), (c) winter (July-September; JAS) and (d) spring (October-December). In areas enclosed by the grey contours nine or more models have the same signed response as the multimodel mean. (e-h) As (a-d), but for mean sea level pressure (MSLP). (i-l) As (a-d), but for 500 hPa westerly wind (U500). The thick black line represents the climatological jet position.

Figure 3: Multi-model-mean inferred zonal-mean air temperature response to Antarctic sea-ice loss in austral (a) summer (January-March; JFM), (b) autumn (April-June; AMJ), (c) winter (July-September; JAS) and (d) spring (October-December). The black contours show the baseline climatology and hatching indicates where nine or more models have the same signed response as the multimodel mean. (e-h) As (a-d), but for zonal-mean westerly wind.

Figure 4: Multi-model-mean inferred jet latitude response to Antarctic sea-ice loss (black line) and the combined response to SST and CO_2 (dashed line) as a function of calendar month. The

right-hand vertical axis (in blue) shows the number of individual models that have the same signed response to sea-ice loss as the multi-model-mean, with filled dots indicating nine or more models agree and stars indicating fewer than nine models agree. (b) As (a), but for jet strength. (c) Jet latitude response to Antarctic sea-ice loss as a function of the climatological jet latitude in the preindustrial control simulation for each model (crosses) and for austral winter (red) and spring (black). Also shown are the linear relationships and their associated correlation coefficients. (d) As (c) but for jet strength.

References

Bader, J., Flügge, M., Kvamstø, N. G., Mesquita, M. D. S., & Voigt, A. (2013). Atmospheric winter response to a projected future Antarctic sea-ice reduction: A dynamical analysis. Climate Dynamics, 40(11–12), 2707–2718. https://doi.org/10.1007/s00382-012-1507-9

Blackport, R., & Kushner, P. J. (2016). The transient and equilibrium climate response to rapid summertime sea ice loss in CCSM4. Journal of Climate, 29(2), 401–417. https://doi.org/10.1175/JCLI-D-15-0284.1

Bracegirdle, T. J., Hyder, P., & Holmes, C. R. (2018). CMIP5 Diversity in Southern Westerly Jet Projections Related to Historical Sea Ice Area: Strong Link to Strengthening and Weak Link to Shift. Journal of Climate, 31(1), 195–211. https://doi.org/10.1175/JCLI-D-17-0320.1

Bracegirdle, T. J., Shuckburgh, E., Sallee, J. B., Wang, Z., Meijers, A. J. S., Bruneau, N., … Wilcox, L. J. (2013). Assessment of surface winds over the atlantic, indian, and pacific ocean sectors of the southern ocean in cmip5 models: Historical bias, forcing response, and state dependence. Journal of Geophysical Research Atmospheres, 118(2), 547–562. https://doi.org/10.1002/jgrd.50153

Ceppi, P., Zappa, G., Shepherd, T. G., & Gregory, J. M. (2018). Fast and slow components of the extratropical atmospheric circulation response to CO2forcing. Journal of Climate, 31(3), 1091–1105. https://doi.org/10.1175/JCLI-D-17-0323.1

Cohen, J., Screen, J. A., Furtado, J. C., Barlow, M., Whittleston, D., Coumou, D., … Jones, J. (2014). Recent Arctic amplification and extreme mid-latitude weather. Nature Geoscience, 7(9), 627–637. https://doi.org/10.1038/ngeo2234

Collins, M., Knutti, R., Arblaster, J., Dufresne, J.-L., Fichefet, T., Friedlingstein, P., … Wehner, M. (2013). Long-term Climate Change: Projections, Commitments and Irreversibility. Climate Change 2013: The Physical Science Basis. Contribution of Working Group I to the Fifth Assessment Report of the Intergovernmental Panel on Climate Change, 1029–1136. https://doi.org/10.1017/CBO9781107415324.024

Deser, C., Tomas, R. A., & Sun, L. (2015). The role of ocean-atmosphere coupling in the zonal-mean atmospheric response to Arctic sea ice loss. Journal of Climate, 28(6), 2168–2186. https://doi.org/10.1175/JCLI-D-14-00325.1

England, M., Polvani, L., & Sun, L. (2018). Contrasting the Antarctic and Arctic atmospheric responses to projected sea ice loss in the late twenty-first century. Journal of Climate, 31(16), 6353–6370. https://doi.org/10.1175/JCLI-D-17-0666.1

Fetterer, F., K. Knowles, W. N. Meier, M. Savoie, and A. K. Windnagel. 2017, updated daily. Sea Ice Index, Version 3.. Boulder, Colorado USA. NSIDC: National Snow and Ice Data Center. doi: https://doi.org/10.7265/N5K072F8.

Holland, M. M., Landrum, L., Kostov, Y., & Marshall, J. (2017). Sensitivity of Antarctic sea ice to the Southern Annular Mode in coupled climate models. Climate Dynamics, 49(5–6), 1813–1831. https://doi.org/10.1007/s00382-016-3424-9

Kidston, J., & E. P. Gerber (2010). Intermodel variability of the poleward shift of the austral jet stream in the CMIP3 integrations linked to biases in 20th century climatology. Geophys. Res. Lett., **37**, L09708, doi:https://doi.org/10.1029/2010GL042873

Kidston, J., Taschetto, A. S., Thompson, D. W. J., & England, M. H. (2011). The influence of Southern Hemisphere sea-ice extent on the latitude of the mid-latitude jet stream. Geophysical Research Letters, 38(15), 1–5. https://doi.org/10.1029/2011GL048056

Kidston, J., Scaife, A. A., Hardiman, S. C., Mitchell, D. M., Butchart, N., Baldwin, M. P., & Gray, L. J. (2015). Stratospheric influence on tropospheric jet streams, storm tracks and surface weather. Nature Geoscience, 8(6), 433–440. https://doi.org/10.1038/NGEO2424

Kim, B. M., Son, S. W., Min, S. K., Jeong, J. H., Kim, S. J., Zhang, X., … Yoon, J. H. (2014). Weakening of the stratospheric polar vortex by Arctic sea-ice loss. Nature Communications, 5, 1–8. https://doi.org/10.1038/ncomms5646

Krinner, G., Largeron, C., Ménégoz, M., Agosta, C., & Brutel-Vuilmet, C. (2014). Oceanic forcing of Antarctic climate change: A study using a stretched-grid atmospheric general circulation model. Journal of Climate, 27(15), 5786–5800. https://doi.org/10.1175/JCLI-D-13-00367.1

Lecomte, O., Goosse, H., Fichefet, T., Holland, P. R., Uotila, P., Zunz, V., & Kimura, N. (2016). Impact of surface wind biases on the Antarctic sea ice concentration budget in climate models. Ocean Modelling, 105, 60–70. https://doi.org/10.1016/j.ocemod.2016.08.001

Ludescher, J., Yuan, N., & Bunde, A. (2018). Detecting the statistical significance of the trends in the Antarctic sea ice extent: an indication for a turning point. Climate Dynamics, 53(1), 237–244. https://doi.org/10.1007/s00382-018-4579-3

Meehl, G. A., Arblaster, J. M., Chung, C. T. Y., Holland, M. M., DuVivier, A., Thompson, L., … Bitz, C. M. (2019). Sustained ocean changes contributed to sudden Antarctic sea ice retreat in late 2016. Nature Communications, 10(1), 14. https://doi.org/10.1038/s41467-018-07865-9

Menéndez, C. G., Serafini, V., & Le Treut, H. (1999). The effect of sea-ice on the transient atmospheric eddies of the Southern Hemisphere. Climate Dynamics, 15(9), 659–671. https://doi.org/10.1007/s003820050308

Peings, Y., & Magnusdottir, G. (2014). Response of the wintertime northern hemisphere atmospheric circulation to current and projected arctic sea ice decline: A numerical study with CAM5. Journal of Climate, 27(1), 244–264. https://doi.org/10.1175/JCLI-D-13-00272.1

Polvani, L. M., & Smith, K. L. (2013). Can natural variability explain observed Antarctic sea ice trends? New modeling evidence from CMIP5. Geophysical Research Letters, 40(12), 3195–3199. https://doi.org/10.1002/grl.50578

Purich, A., Cai, W., England, M. H., & Cowan, T. (2016). Evidence for link between modelled trends in Antarctic sea ice and underestimated westerly wind changes. Nature Communications, 7(May 2015), 10409. https://doi.org/10.1038/ncomms10409

Raphael, M. N., Hobbs, W., & Wainer, I. (2011). The effect of Antarctic sea ice on the Southern Hemisphere atmosphere during the southern summer. Climate Dynamics, 36(7), 1403–1417. https://doi.org/10.1007/s00382-010-0892-1

Roach, L. A., Dean, S. M., & Renwick, J. A. (2018). Consistent biases in Antarctic sea ice concentration simulated by climate models. Cryosphere, 12(1), 365–383. https://doi.org/10.5194/tc-12-365-2018

Schlosser, E., Haumann, F. A., & Raphael, M. N. (2017). Atmospheric influences on the anomalous 2016 Antarctic sea ice decay. The Cryosphere Discussions, 13(3), 1–31. https://doi.org/10.5194/tc-2017-192

Schroeter, S., Hobbs, W., & Bindoff, N. L. (2017). Interactions between Antarctic sea ice and large-scale atmospheric modes in CMIP5 models. The Cryosphere, 11(2), 789–803. https://doi.org/10.5194/tc-11-789-2017

Screen, James A., Deser, C., Smith, D. M., Zhang, X., Blackport, R., Kushner, P. J., … Sun, L. (2018). Consistency and discrepancy in the atmospheric response to Arctic sea-ice loss across climate models. Nature Geoscience, 11(3), 155–163. https://doi.org/10.1038/s41561-018-0059-y

Screen, James A., & Simmonds, I. (2013). Exploring links between Arctic amplification and mid-latitude weather. Geophysical Research Letters, 40(5), 959–964. https://doi.org/10.1002/grl.50174

Screen, James A., Simmonds, I., Deser, C., & Tomas, R. (2013). The atmospheric response to three decades of observed arctic sea ice loss. Journal of Climate, 26(4), 1230–1248. https://doi.org/10.1175/JCLI-D-12-00063.1

Smith, D. M., Dunstone, N. J., Scaife, A. A., Fiedler, E. K., Copsey, D., & Hardiman, S. C. (2017). Atmospheric response to Arctic and Antarctic sea ice: The importance of ocean-atmosphere coupling and the background state. Journal of Climate, 30(12), 4547–4565. https://doi.org/10.1175/JCLI-D-16-0564.1

Stuecker, M. F., Bitz, C. M., & Armour, K. C. (2017). Conditions leading to the unprecedented low Antarctic sea ice extent during the 2016 austral spring season. Geophysical Research Letters, 1–12. https://doi.org/10.1002/2017GL074691

Turner, J., Bracegirdle, T. J., Phillips, T., Marshall, G. J., & Scott Hosking, J. (2013). An initial assessment of antarctic sea ice extent in the CMIP5 models. Journal of Climate, 26(5), 1473–1484. https://doi.org/10.1175/JCLI-D-12-00068.1

Turner, J., Phillips, T., Marshall, G. J., Hosking, J. S., Pope, J. O., Bracegirdle, T. J., & Deb, P. (2017). Unprecedented springtime retreat of Antarctic sea ice in 2016. Geophysical Research Letters, 44(13), 6868–6875. https://doi.org/10.1002/2017GL073656

Vaughan, D. G. J. C. C. (2013). Observations: Cryosphere. Climate Change 2013 the Physical Science Basis: Working Group I Contribution to the Fifth Assessment Report of the Intergovernmental Panel on Climate Change, 9781107057, 317–382. https://doi.org/10.1017/CBO9781107415324.012

Vavrus, S. J. (2018). The Influence of Arctic Amplification on Mid-latitude Weather and Climate. Current Climate Change Reports, 4(3), 238–249. https://doi.org/10.1007/s40641-018-0105-2

Wang, G., Hendon, H. H., Arblaster, J. M., Lim, E.-P., Abhik, S., & van Rensch, P. (2019). Compounding tropical and stratospheric forcing of the record low Antarctic sea-ice in 2016.

Nature Communications, 10(1), 13. https://doi.org/10.1038/s41467-018-07689-7

Zappa, G., Pithan, F., & Shepherd, T. G. (2018). Multimodel Evidence for an Atmospheric Circulation Response to Arctic Sea Ice Loss in the CMIP5 Future Projections. Geophysical Research Letters, 45(2), 1011–1019. https://doi.org/10.1002/2017GL076096

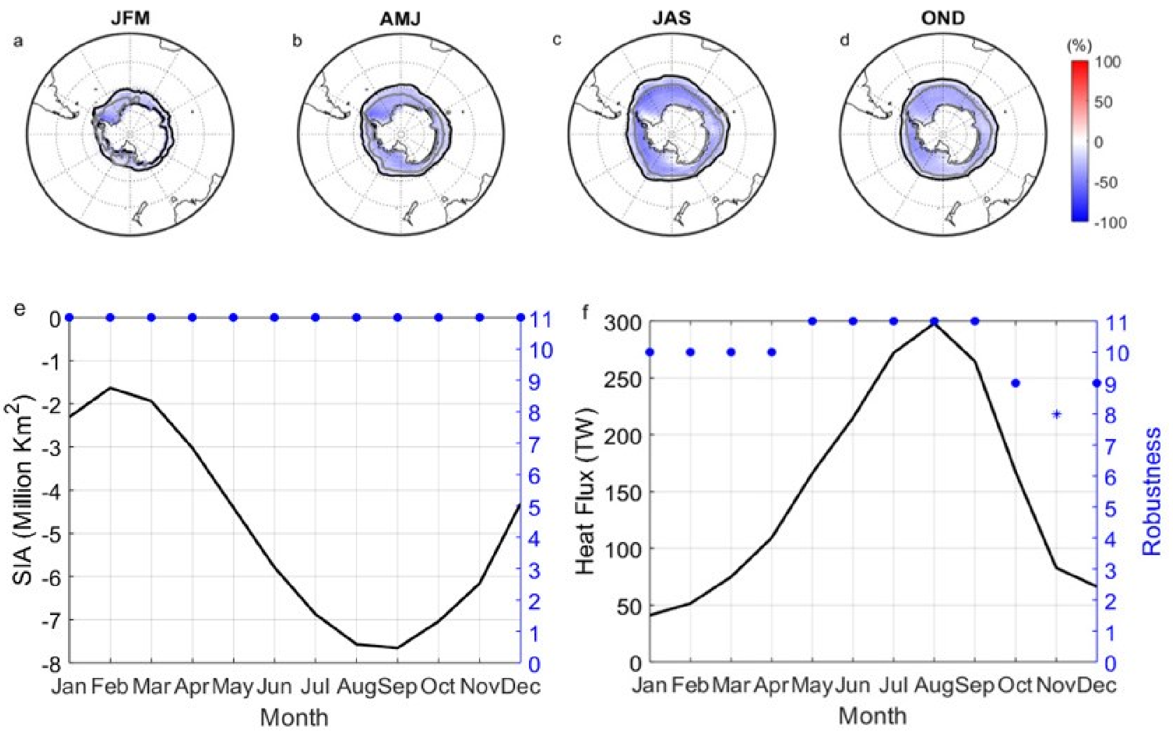

Figure 1: Multi-model-mean sea ice concentration response to quadrupled CO_2 in austral (a) summer (January-March; JFM), (b) autumn (April-June; AMJ), (c) winter (July-September; JAS) and (d) spring (October-December). The black and grey contours show the sea-ice edge (15% concentration) in the quadrupled and control simulations, respectively. (e) Multi-model-mean sea-ice area (SIA) response to quadrupled CO_2 as a function of calendar month. The right-hand vertical axis (in blue) shows the number of models that have the same signed response as the multimodel mean, with filled dots indicating nine or more models have the same signed response as the multimodel mean and stars indicating fewer than nine models have the same signed response as the multimodel mean. (f) As (e), but for the inferred surface turbulent heat flux response, calculated as the area-weighted surface turbulent (sensible plus latent) heat flux response, summed over Southern Hemisphere grid points where the sea-ice concentration differs between the preindustrial and quadrupled CO_2 states. The heat flux is defined as positive in the upward direction.

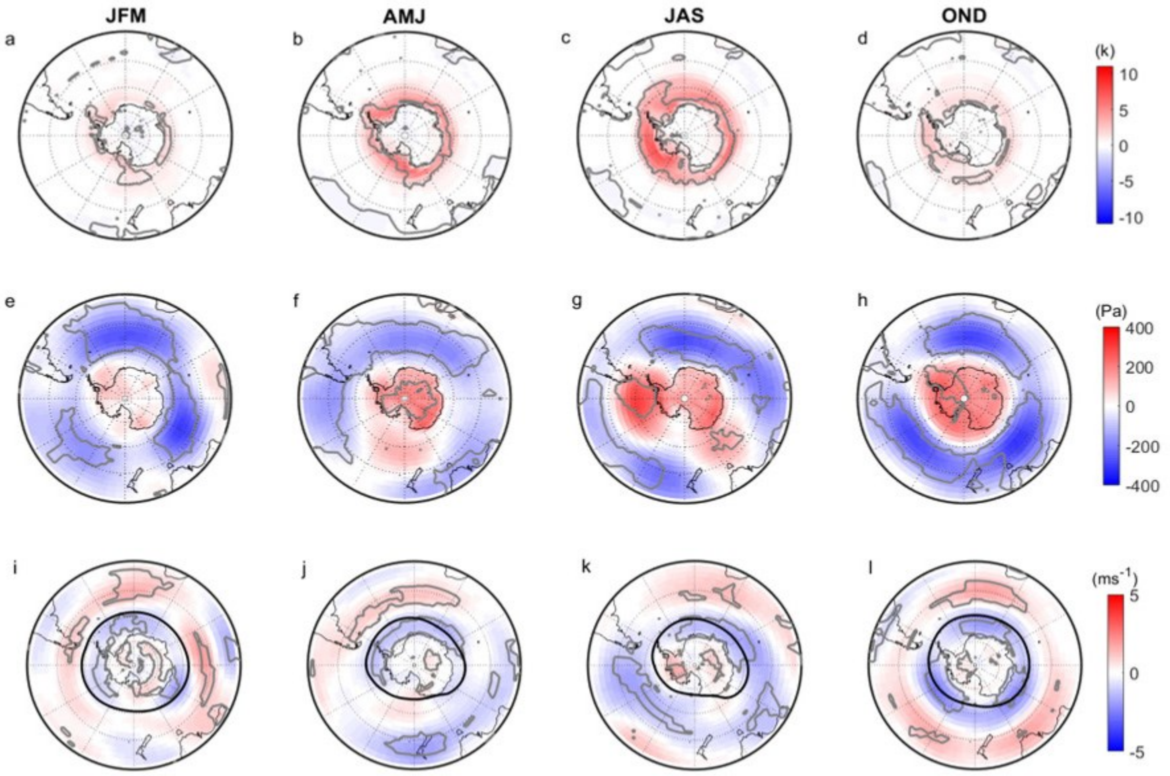

Figure 2: Multi-model-mean inferred surface air temperature (TAS) response to Antarctic sea-ice loss in austral (a) summer (January-March; JFM), (b) autumn (April-June; AMJ), (c) winter (July-September; JAS) and (d) spring (October-December). In areas enclosed by the grey contours nine or more models have the same signed response as the multimodel mean. (e-h) As (a-d), but for mean sea level pressure (MSLP). (i-l) As (a-d), but for 500 hPa westerly wind (U500). The thick black line represents the climatological jet position.

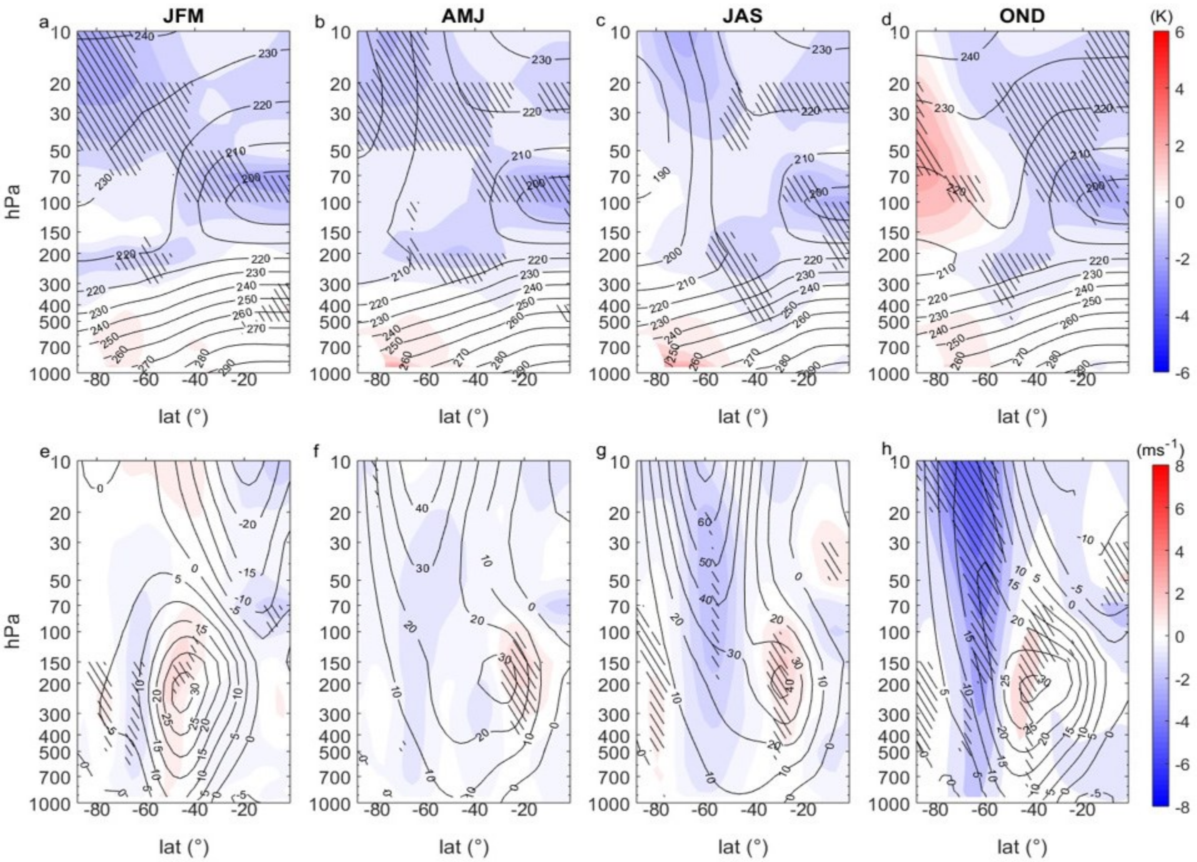

Figure 3: Multi-model-mean inferred zonal-mean air temperature response to Antarctic sea-ice loss in austral (a) summer (January-March; JFM), (b) autumn (April-June; AMJ), (c) winter (July-September; JAS) and (d) spring (October-December). The black contours show the baseline climatology and hatching indicates where nine or more models have the same signed response as the multimodel mean. (e-h) As (a-d), but for zonal-mean westerly wind.

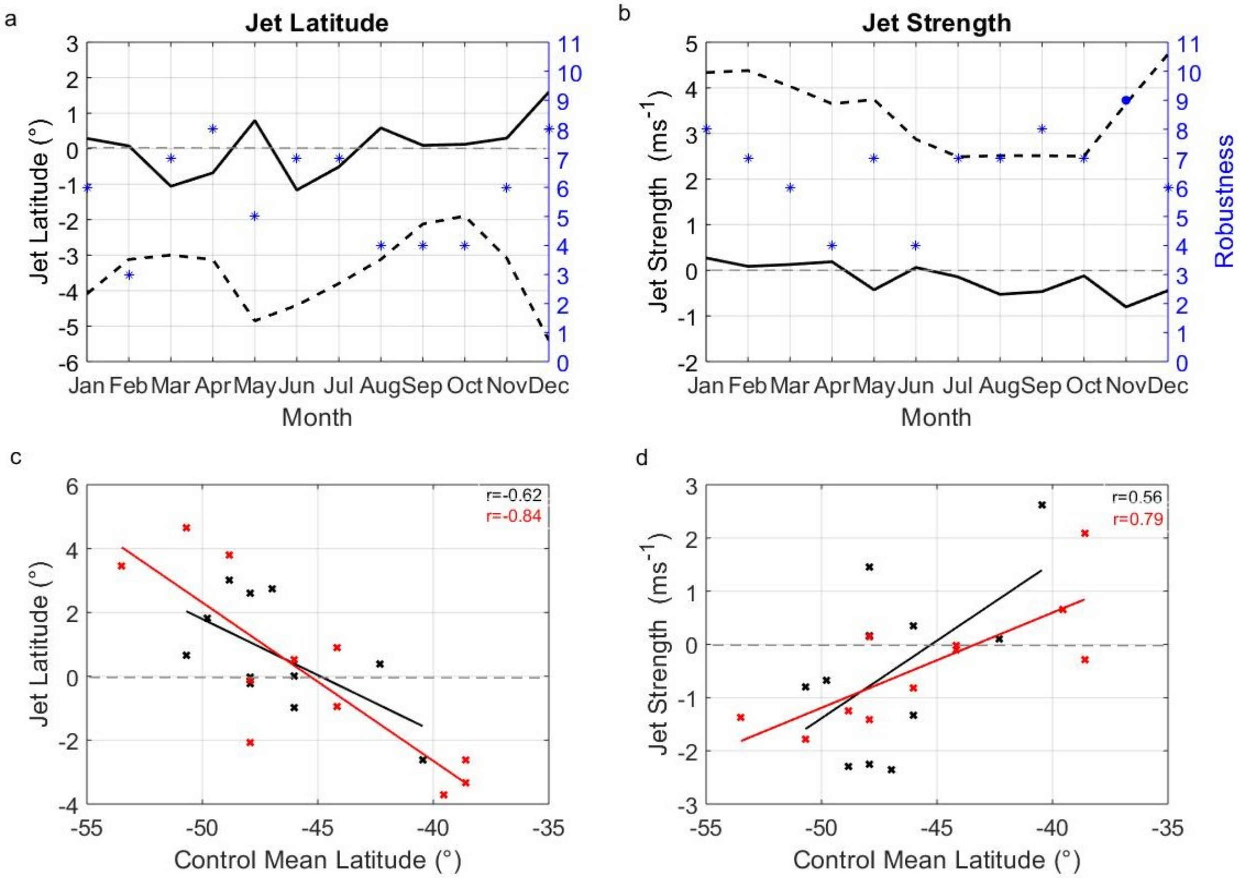

Figure 4: Multi-model-mean inferred jet latitude response to Antarctic sea-ice loss (black line) and the combined response to SST and CO_2 (dashed line) as a function of calendar month. The right-hand vertical axis (in blue) shows the number of individual models that have the same signed response to sea-ice loss as the multi-model-mean, with filled dots indicating nine or more models agree and stars indicating fewer than nine models agree. (b) As (a), but for jet strength. (c) Jet latitude response to Antarctic sea-ice loss as a function of the climatological jet latitude in the preindustrial control simulation for each model (crosses) and for austral winter (red) and spring (black). Also shown are the linear relationships and their associated correlation coefficients. (d) As (c) but for jet strength.